Temperature-insensitive miniaturized fiber inline Fabry-Perot interferometer for highly sensitive refractive index measurement

Tao Wei,[1] Yukun Han,[2] Yanjun Li, [1] Hai-Lung Tsai,[2] and Hai Xiao[1*]

[1]*Department of Electrical and Computer Engineering,*
[2]*Department of Mechanical and Aerospace Engineering,*
Missouri University of Science and Technology, 1870 Miner Circle, Rolla, MO 65409-0040, USA
[*]*Corresponding author: xiaoha@mst.edu*

Abstract: We report a miniaturized fiber inline Fabry-Perot interferometer (FPI), with an open micro-notch cavity fabricated by one-step fs laser micromachining, for highly sensitive refractive index measurement. The device was tested for measurement of the refractive indices of various liquids including isopropanol, acetone and methanol at room temperature, as well as the temperature-dependent refractive index of deionized water from 3 to 90°C. The sensitivity for measurement of refractive index change of water was 1163 nm/RIU at the wavelength of 1550 nm. The temperature cross-sensitivity of the device was about 1.1×10^{-6} RIU/°C. The small size, all-fiber structure, small temperature dependence, linear response and high sensitivity, make the device attractive for chemical and biological sensing.

OCIS codes: (060.2370) Fiber optics sensors; (060.2340) Fiber optics components; (120.2230) Fabry-Perot.

References and links

1. I. Del Villar, I. R. Matias, and F. J. Arregui, "Enhancement of sensitivity in long-period fiber gratings with deposition of low-refractive-index materials," Opt. Lett. **30**, 2363-2365 (2005).
2. W. Liang, Y. Huang, Y. Xu, R. K. Lee, and A. Yariv, "Highly sensitive fiber Bragg grating refractive index sensors," Appl. Phys. Lett. **86**, 151122:1-3 (2005).
3. I. M. White, H. Oveys, and X. Fan, "Liquid-core optical ring-resonator sensors," Opt. Lett. **31**, 1319-1321 (2006).
4. B. Gauvreau, A. Hassani, M. Fassi Fehri, A. Kabashin, and M. A. Skorobogatiy, "Photonic bandgap fiber-based Surface Plasmon Resonance sensors," Opt. Express **15**, 11413-11426 (2007).
5. N. Skivesen, A. Tetu, M. Kristensen, J. Kjems, L. H. Frandsen, and P. I. Borel, "Photonic-crystal waveguide biosensor," Opt. Express **15**, 3169-3176 (2007).
6. I. M. White and X. Fan, "On the performance quantification of resonant refractive index sensors," Opt. Express **16**, 1020-1028 (2008).
7. Y. J. Rao, "Recent progress in fiber-optic extrinsic Fabry-Perot interferometric sensors," Opt. Fiber Technol. **12**, 227-237 (2006).
8. V. Bhatia, K. A. Murphy, R. O. Claus, M. E. Jones, J. L. Grace, T. A. Tran, and J. A. Greene, "Optical fiber based absolute extrinsic Fabry - Perot interferometric sensing system," Meas. Sci. Technol. **7**, 58-61 (1996).
9. H. Xiao, J. Deng, G. Pickrell, R. G. May, and A. Wang, "Single-crystal sapphire fiber-based strain sensor for high-temperature applications," J. Lightwave Technol. **21**, 2276-2283 (2003).
10. Y. Zhang, X. Chen, Y. Wang, K. L. Cooper, and A. Wang, "Microgap Multicavity Fabry–Pérot Biosensor," J. Lightwave Technol. **25**, 1797-1804 (2007).
11. G. Z. Xiao, A. Adnet, Z. Y. Zhang, F. G. Sun, and C. P. Grover, "Monitoring changes in the refractive index of gases by means of a fiber optic Fabry-Perot interferometer sensor," Sensor Actuat. A-Phys. **118**, 177-182 (2005).
12. Z. L. Ran, Y. J. Rao, W. J. Liu, X. Liao, and K. S. Chiang, "Laser-micromachined Fabry-Perot optical fiber tip sensor for high-resolution temperature-independent measurement of refractive index," Opt. Express **16**, 2252-2263 (2008).
13. Y. J. Rao, M. Deng, D. W. Duan, X. C. Yang, T. Zhu, and G. H. Cheng, "Micro Fabry-Perot interferometers in silica fibers machined by femtosecond laser," Opt. Express **15**, 14123-14128 (2007).
14. Z. L. Ran, Y. J. Rao, H. Y. Deng, and X. Liao, "Miniature in-line photonic crystal fiber etalon fabricated by 157 nm laser micromachining," Opt. Lett. **32**, 3071-3073 (2007).

#93750 - $15.00 USD Received 11 Mar 2008; revised 7 Apr 2008; accepted 7 Apr 2008; published 10 Apr 2008

15. T. Wei, Y. Han, H-L. Tsai, and H. Xiao, "Miniaturized fiber inline Fabry-Perot interferometer fabricated with a femtosecond laser," Opt. Lett. **33**, 536-538 (2008).
16. B. Qi, G. R. Pickrell, J. Xu, P. Zhang, Y. Duan, W. Peng, Z. Huang, W. Huo, H. Xiao, R. G. May, and A. Wang, "Novel data processing techniques for dispersive white light interferometer," Opt. Eng. **42**, 3165-3171 (2003).
17. J. B. Hawkes, and R. W. Astherimer, "Temperature coefficient of the refractive index of water," J. Opt. Soc. Am. **38**, 804-806 (1948).

1. Introduction

Miniaturized and robust optical sensors capable of accurate and reliable measurement of refractive index of liquids have attracted tremendous interest in recent years due to their broad applications in chemical and biological sensing. Preferably, these devices shall have a small size, high sensitivity, fast response time and large dynamic range. Many existing devices operate based on evanescent field interactions. Examples include long period fiber gratings (LPFG) [1], chemically etch-eroded fiber Bragg gratings (FBG) [2], optical microresonators/ microcavities [3], fiber surface plasmon resonance (SPR) devices [4], photonic crystals [5], etc. In general, these devices have shown high sensitivity for refractive index measurement. Characterized as the resonance wavelength shift in response to refractive index changes, it has been reported that LPFGs can provide a sensitivity as high as 6000 nm/RIU (refractive index unit) while microresonators can reach 800 nm/RIU [6]. However, the evanescent field-based devices have a nonlinear response to refractive index, meaning that the sensitivity varies at different refractive index ranges. The dynamic range of refractive index measurement is also limited. In addition, many existing devices have shown large temperature cross-sensitivity. As a result, temperature variation induced errors need to be corrected in real time.

Low finesse fiber Fabry-Perot interferometers (FPI) have been widely used as optical sensors for measurement of a variety of parameters such as pressure, strain, temperature, etc. [7]. However, they have been commonly made with a sealed cavity. [8-10] As a result, their applications have been mainly limited to the measurement of physical parameters. In a fiber FPI, the phase of the interference signal is linearly proportional to the optical length of the cavity, defined as the product of the cavity length and the refractive index of the medium filling the cavity. When exposed to the external environment, a FPI cavity can be used to measure the refractive index change with a linear response by tracking the phase shift of the interference signal. Compared with other types of sensors, a FPI refractive index sensor has the unique advantage of constant sensitivity over a large dynamic range. Xiao, *et al*., reported a FPI refractive index sensor formed by two polished fiber endfaces hosted in a holey sleeve [11]. The holey sleeve allows gas to freely enter and leave the cavity. A resolution of 10^{-5} was estimated in monitoring the changes in the refractive index of gases. However, the sensor assembly was complicated and required the use of epoxy and various components made of different materials. As a result, the device had a strong dependence on temperature. Recently, Ran, *et al*., described a refractive index sensor by adding a sealed Fabry-Perot cavity near the tip of a single-mode fiber [12]. In this case, the sealed FPI itself was not a sensing device and only served as a signal modulator. The external refractive index variation changed the reflectivity of the exposed fiber tip. The variation of the maximum contrast of the interference fringes was used to determine the amount of refractive index change. The device had a refractive index resolution of $\sim 4\times10^{-5}$.

Recently, Rao, *et al*., reported a miniaturized fiber inline FPI device fabricated by micromachining a rectangular non-through hole into a single-mode or photonic crystal fiber using a femtosecond (fs) laser [13]. The single-mode fiber FPI device had a fringe visibility of about 2 dB. Later, a 157 nm laser was used to improve the quality of fabrication and a 26 dB fringe visibility was obtained using a photonic crystal fiber which had a strong absorption at the wavelength of 157 nm [14]. Our group also demonstrated an inline FPI device with a fringe visibility of 16 dB by fs laser one-step micromachining a micro-notch on a single-mode fiber [15]. The all-glass structured inline FPI has very small temperature dependence and more attractively, an open micro-notch cavity that allows prompt access to liquid samples for

#93750 - $15.00 USD Received 11 Mar 2008; revised 7 Apr 2008; accepted 7 Apr 2008; published 10 Apr 2008

direct refractive index measurement. In this paper, we report our experimental investigations on its capability for temperature-insensitive refractive index sensing.

2. Sensor fabrication and principle of operation

Figure 1 shows the structural schematic, the scanning electron microscope (SEM) image, and the simulated interference spectrum of the fiber inline FPI device. The device was made by machining a micro-notch on a single-mode fiber using a fs laser (Legend-F, Coherent, Inc.) with a repetition rate, center wavelength, and pulse width of 1 kHz, 800 nm and 120 fs, respectively [15]. The cavity length was about 60 μm as estimated from the SEM image. The defects shown in the picture were caused by too large a laser power and were eliminated by reducing the laser power. The depth of the micro-notch was around 72 μm, just passing the fiber core. The FPI cavity was made very close (~2 mm) to the end of the fiber. With such a short bending arm, the chance of bending induced device breakage is small.

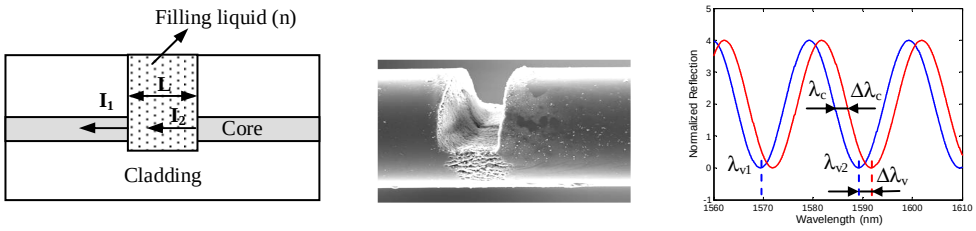

(a) (b) (c)

Fig. 1. Fiber inline FPI fabricated by fs laser micromachining, (a) structural schematic, (b) SEM image, and (c) simulated interference spectrum.

Due to the low reflectivity of the laser-ablated surface, multiple reflections have negligible contributions to the optical interference. The low finesse FP device can thus be modeled using the two-beam optical interference equation [16]:

$$I = I_1 + I_2 + 2\sqrt{I_1 I_2}\cos\left(\frac{4\pi n \cdot L}{\lambda} + \phi_0\right) \tag{1}$$

where, I is the intensity of the interference signal; I_1 and I_2 are the reflections at the cavity endfaces, respectively; φ_0 is the initial phase of the interference; L is the cavity length; n is the refractive index of the medium filling the cavity; λ is the optical wavelength in vacuum.

According to Eq. (1), the interference signal reaches its minimum (I_{min}) when the phase of the cosine term becomes an odd number of π. That is

$$I = I_{\min}, \qquad \text{when} \quad \frac{4\pi n \cdot L}{\lambda_v} + \phi_0 = (2m+1)\pi \tag{2}$$

where *m* is an integer and λ_v is the center wavelength of the specific interference valley.

The two adjacent interference minimums have a phase difference of 2π. Therefore the optical length of the cavity can be calculated by:

$$L \cdot n = \frac{1}{2}\left(\frac{\lambda_{v1}\lambda_{v2}}{\lambda_{v2} - \lambda_{v1}}\right) \tag{3}$$

where λ_{v1} and λ_{v2} are the center wavelengths of two adjacent valleys [Fig. 1(c)] in the interference spectrum. In theory, Eq. (3) can be used to calculate either the absolute refractive index (n) or the absolute length (L) of the cavity if one of them is known. However, the measurement based on Eq. (3) has a poor resolution because the period is not a sensitive function of the optical path change [11, 16].

In many cases, only the relative refractive index change is of interest and the range of refractive index variation is small so the phase shift is less than 2π. In this case, the phase

#93750 - $15.00 USD Received 11 Mar 2008; revised 7 Apr 2008; accepted 7 Apr 2008; published 10 Apr 2008

ambiguity issue can be avoided. The relative refractive index change can be calculated based on the spectral shift of the interferogram.

In Eq. (2), taking the derivative of n with respect to λ_v, one finds:

$$\frac{dn}{d\lambda_v} = \frac{1}{4\pi L} \quad . \tag{4}$$

Assuming the cavity length is maintained constant during measurement, the amount of refractive index change (Δn) can be computed based on the wavelength shift [$\Delta\lambda_v$ as shown in Fig. 1(c)] of a particular interference valley using the following equation derived based on Eq. (4):

$$\Delta n = \frac{\Delta\lambda_v}{\lambda_v} n \, , \tag{5}$$

where the relative refractive index change is directly proportional to the spectral shift of the interferogram. It is worth noting that Eq. (5) is also applicable to other characteristic spectral positions such as the interference peak and the center point of the interferogam (λ_c and $\Delta\lambda_c$ in Fig. 1(c) where the curve is relatively linear). The advantage of using the center point in calculation is that its spectral position can be resolved with a higher resolution compared to the valley or the peak that typically has a flat bottom or top. In addition, curve fitting of the interference fringe can also improve the measurement accuracy.

Comparing Eqs. (3) and (5), one finds that Eq. (3) can be used to calculate the absolute refractive index while Eq. (5) only provides the relative change of the refractive index. However, the calculation based on Eq. (5) has a much higher resolution than that obtained using Eq. (3). When used to monitor the relative refractive index change of water with a nominal refractive index of 1.333, the sensitivity of measurement is 1163 nm/RIU at the wavelength of 1550 nm according to Eq. (5). The actual detection limit depends directly on the resolution with which the spectral shift of the interferogram can be determined. If a resolution of 10 pm is achieved in the determination of interferogram shift, a detection limit of 8.6×10^{-6} RIU is attainable. With a rough resolution of 1 nm, the detection limit of 8.6×10^{-4} RIU can still be achieved.

3. Experiment and discussion

The interference spectrum of the fabricated device in air at room temperature is shown in Fig. 2. The loss of this particular device was about 20 dB higher than that of a FPI formed by cleaved fiber endfaces. The interference spectrum indicated a fringe visibility of about 5 dB, which was sufficient for most sensing applications. The length of the FPI cavity was found to be 63.144 μm using Eq. (3) with n set to be 1.0003 for air at the wavelength of 1550 nm [11]. The calculated value was very close to the cavity length estimated by the SEM image.

To evaluate its capability for refractive index measurement, the fiber FPI device was tested using various liquids including methanol, acetone and isopropanol at room temperature. The interrogation of the FPI sensor is schematically shown in Fig. 3. A broadband source made by multiplexing a C-band (AFC, BBS-1550A-TS) and an L-band (Highwave, HWT-BS-L-P) erbium-doped fiber amplified-spontaneous-emission (ASE) source was used to excite the device through a 3 dB fiber coupler. The reflected interference signal from the sensor was detected by an optical spectrum analyzer (OSA, HP70952B). The spectral resolution of OSA was set to 0.5 nm and 1600 data points were obtained per OSA scan.

The interference spectra of the device immersed in various liquids are also shown in Fig. 2 for comparison. The signal intensity dropped when the device was immersed in liquids as a result of the reduced refractive index contrast and thus lower Fresnel reflections from the cavity endfaces. However, the interference fringes maintained a similar visibility. The spectral distance between the two adjacent valleys also decreased, indicating the increase of refractive index of the medium inside the cavity. Using Eq. (3), the refractive indices of the liquids were calculated to be: $n_{methanol} = 1.3283$, $n_{acetone} = 1.3577$, and $n_{isopropanol} = 1.3739$, which were close to the commonly accepted values.

#93750 - $15.00 USD Received 11 Mar 2008; revised 7 Apr 2008; accepted 7 Apr 2008; published 10 Apr 2008

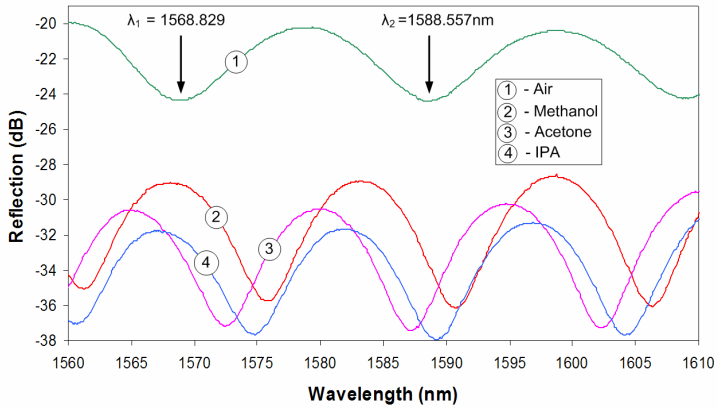

Fig. 2. Interference spectra of the FPI device in air, methanol, acetone and isopropanol.

We also studied the device's capability for temperature-insensitive refractive index sensing by measuring the temperature-dependent refractive index of deionized water. As shown in Fig. 3, the fiber FPI device was attached to the tip of a thermometer and immersed into deionized water in a beaker. The beaker is placed in a large container for water/ice bath and the container was placed on a stirring/hot plate (Corning PC-420D). A magnetic stirrer was used to equilibrate the temperature during experiment. The system was first heated till the water inside the beaker reached 90°C read from the thermometer. Then the heater was turned off to allow the system to cool down smoothly while the interference spectrum was recorded at every degree centigrade of temperature dropping. Ice was added into the water-bath container to help cool the system at low temperatures. The measurement ended till the temperature inside the beaker dropped to 3°C.

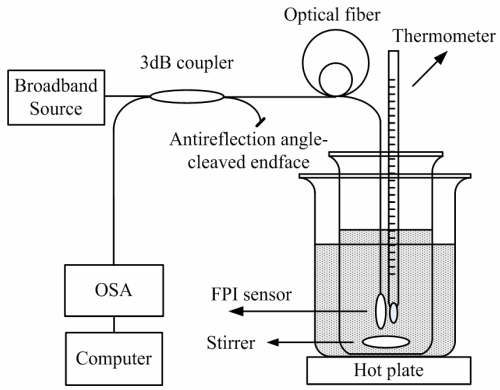

Fig. 3. Experimental setup for refractive index measurement.

Figure 4 shows the measured refractive index of deionized water as a function of temperature. As the temperature increases, the interference fringe shifts to a shorter wavelength indicating the decrease in its refractive index. Assuming a constant cavity length over the entire temperature range, we calculated the refractive index change using Eq. (5) by tracing the spectral shift of the interferogram. To improve the accuracy of spectral shift measurement, the interference fringes were first normalized to have the same average intensities, then curve-fitted using a fourth-order polynomial. The spectral shift was computed as the difference in wavelength between the two fitted curves at the center point.

To achieve an improved resolution, a relative measurement method was used. We first computed the change in refractive index from 20°C to a specific temperature using Eq. (5) based on the spectral shift in their interferograms. The change was then added to the refractive

#93750 - $15.00 USD Received 11 Mar 2008; revised 7 Apr 2008; accepted 7 Apr 2008; published 10 Apr 2008

index value at 20°C to calculate the refractive index of water at that temperature. Point-by-point, the refractive indices of deionized water at various temperatures were obtained. The measurement results, as shown in Fig. 4, indicate that the refractive index of water decreases nonlinearly as its temperature increases. The amount and shape of the measured refractive index of water change as a function of temperature agreed well with the previously reported measurement data [17].

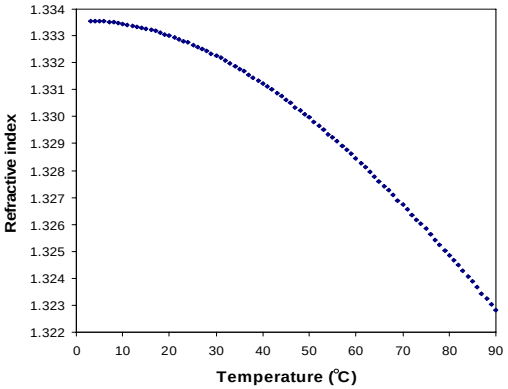

Fig. 4. Measured refractive index of deionized water as a function of temperature.

The above measurement results also included the error contribution of the temperature cross-sensitivity of the device. To evaluate the temperature cross-sensitivity of the sensor, we conducted an experiment in which the sensor was placed in an electrical oven and the temperature of the oven was increased from 20 to 100°C. The 80°C temperature variation in air caused a total interferogram shift in the amount less than 0.1 nm, or at a rate less than 0.00125 nm/°C. Based on Eq. (5), the temperature cross-sensitivity of the device was less than 1.1×10^{-6} RIU/°C. Therefore, the total temperature cross-sensitivity induced measurement error was less than 9.4×10^{-5} RIU in Fig. 4 over the temperature variation of 87°C. The temperature dependence of the device was small and contributed only about 0.9% to the total refractive index variation over the entire temperature range.

4. Conclusion

In conclusion, we demonstrated a miniaturized fiber inline FPI device with an open cavity fabricated by one-step fs laser micromachining for highly sensitive refractive index measurement. The device was evaluated for refractive index measurement of various liquids and the results matched well with the reported data. The inline fiber FPI was also tested to measure the temperature-dependent refractive index of deionized water from 3 to 90°C with a sensitivity of 1163 nm/RIU. The temperature cross-sensitivity of the device was less than 1.1×10^{-6} RIU/°C. The small size, all-fiber inline structure, small temperature dependence, linear response, high sensitivity, and most attractively, an open cavity that is accessible to the external environment, make the new fiber inline FPI an attractive refractive index sensor that has many applications in chemical and biological sensing.

Acknowledgment

The research work was supported by the Office of Naval Research through the Young Investigator Program (N00014-07-0008) and the University of Missouri Research Board (UMRB).

#93750 - $15.00 USD Received 11 Mar 2008; revised 7 Apr 2008; accepted 7 Apr 2008; published 10 Apr 2008